耦合区数量对鼎形微环谐振器输出的影响

吴蓉 张皓辰

The influence of the number of coupling regions on the output of the ding-shaped microring resonator

WU Rong, ZHANG Hao-chen

引用本文:
吴蓉, 张皓辰. 耦合区数量对鼎形微环谐振器输出的影响[J]. 中国光学, 2023, 16(6): 1493–1500. doi: 10.37188/CO.EN–2023–0009
WU Rong, ZHANG Hao-chen. The influence of the number of coupling regions on the output of the ding-shaped microring resonator[J]. *Chinese Optics*, 2023, 16(6): 1493-1500. doi: 10.37188/CO.EN-2023-0009

在线阅读 View online: https://doi.org/10.37188/CO.EN–2023–0009

中国光学（中英文）
Chinese Optics

文章编号 2097-1842(2023)06-1493-08

The influence of the number of coupling regions on the output of the ding-shaped microring resonator

WU Rong, ZHANG Hao-chen*

(*School of Electronic and Information Engineering*, *Lanzhou Jiaotong University*, *Lanzhou* 730070, *China*)

* *Corresponding author*, *E-mail*: 2651809834@qq.com

Abstract: In order to explore the influence of the number of coupling regions on the output of the ding-shaped microring resonator, the physical model of the ding-shaped microring resonator is established and studied by using the transfer matrix method. On this basis, the influence of the number of different coupling regions on the output of the ding-shaped microring resonator is analyzed. The experimental results show that with the increase of the number of coupling regions, the number of resonance peaks increases in the range of 1.54~1.56 μm working wavelength, the full width at half maximum (FWHM) decreases, the quality factor Q increases, the energy storage performance of the device is better, and the filter function on a specific wavelength can be realized. It can be concluded that the number of coupling regions has a great influence on the performance of the ding-shaped microring resonator. The number of coupling regions is selected according to the actual needs in the design.

Key words: ding-shaped microring resonator; number of coupling regions; transfer matrix; high transmittance

耦合区数量对鼎形微环谐振器输出的影响

吴　蓉，张皓辰*

（兰州交通大学 电子与信息工程学院，甘肃 兰州 730070）

摘要：为了探究鼎形微环谐振器的耦合区数量对输出的影响，建立了鼎形微环谐振器的物理模型。利用传输矩阵法对鼎形微环谐振器的物理模型进行研究。分析了不同耦合区数量对鼎形微环谐振器输出的影响。实验结果表明，随着耦合区数量的增加，在 1.54~1.56 μm 工作波长范围内谐振峰的数量增加，半高全宽 FWHM 越小，品质因子 Q 则越大，器件的储能性能越好，并且还能实现对特定波长的滤波作用。耦合区数量对鼎形微环谐振器性能有着很大影响，在设计时根据实际需要选择耦合区数量。

关　键　词：鼎形微环谐振器；耦合区数量；传输矩阵；高透射率

中图分类号：TN256　　**文献标志码：**A　　**doi:** 10.37188/CO.EN-2023-0009

收稿日期：2023-04-25；**修订日期：**2023-05-26

基金项目：甘肃省自然科学基金（No. 21JR7RA289）

Supported by Natural Science Foundation of Gansu Province (No. 21JR7RA289)

1 Introduction

Since Marcatili A J[1] proposed the concept of microring resonator in 1969, the research on the structure of microring resonator has been carried out for many years[2-6]. The structure of the ding-shaped microring resonator was first proposed by Canadian scholar Sacher W D[7] *et al*. in 2014. Due to the large number of coupling regions of the ding-shaped microring resonator, the transmission loss is large and the increase in the number of coupling regions leads to an increase in the volume of the ding-shaped microring resonator. There are relatively few applications and researches on the ding-shaped microring resonator, mainly focusing on filtering and phase shift.

2 Fundamental theory

The ding-shaped microring resonator is the deformation of the dual-channel microring resonator. The difference is that the dual-channel microring resonator has only two coupling regions, and the standard ding-shaped microring resonator is based on the dual-channel microring resonator. In order to increase the number of coupling regions, the shape of the straight waveguide and the ring waveguide is adjusted, so that four coupling regions are formed, which greatly improves the selectivity of the ding-shaped microring resonator to specific wavelengths of light. As shown in Fig.1, C_1, C_2, C_3 and C_4 represent four coupling regions respectively, and CW_1 and CW_2 represent two curved waveguides.

In this paper, by adjusting the number of coupling regions of the standard ding-shaped microring resonator, the influence of the number of coupling regions on the output spectrum is observed. The physical model of the ding-shaped microring resonator with different numbers of coupling regions is analyzed. The output spectrum and field of the ding-shaped microring resonator are analyzed.Since the basic structure of the ding-shaped microring resonator is a directional coupler, the ding-shaped microring resonator model is analyzed by using the transfer matrix[8-10], and the influence of the number of coupling regions on the output of the ding-shaped microring resonator is studied. The coupler structure is shown in Fig.2.

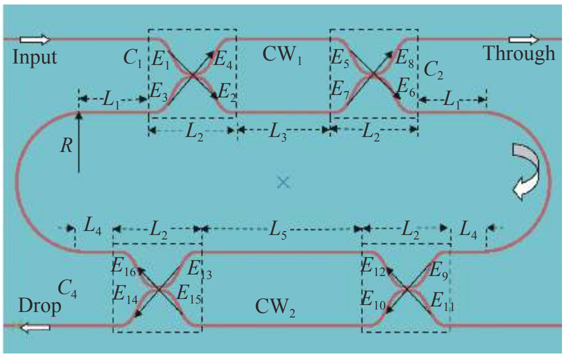

Fig. 1 Physical model of standard ding-shaped microring resonator

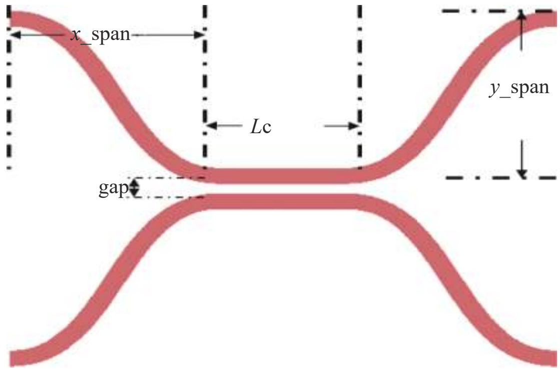

Fig. 2 The model of the coupler

By the transfer matrix method, the transfer matrix relationship of the coupling region C_1 can be expressed as :

$$\begin{pmatrix} E_4 \\ E_2 \end{pmatrix} = \begin{pmatrix} t_1 & k_1 \\ -k_1^* & t_1^* \end{pmatrix} \begin{pmatrix} E_1 \\ E_3 \end{pmatrix} , \qquad (1)$$

where E_2, E_4 represent the complex amplitudes generated when the output coupling region is C_1; E_1, E_3 represent the complex amplitudes generated when the input coupling region is C_1; t_1, t_1^* are the self-coupling coefficients of the coupling regions C_1, and k_1, k_1^* are the cross-coupling coefficients of the coupling region C_1.

As for the uncoupled region C_2, there are:

$$E_5 = \exp[-j(\varphi_1 + \Delta\varphi_1)]E_1 \quad , \qquad (2)$$

$$E_7 = \exp[-j(\varphi_2 + \Delta\varphi_2)]E_2 \quad . \qquad (3)$$

In the above formulas, E_5 and E_7 are the complex amplitudes generated when the input coupling region is C_2; φ_1, φ_2 are the phase changes in the phase shifter and they meet $\varphi_1 + \Delta\varphi_1 = -(\varphi_2 + \Delta\varphi_2)$.

Similarly, the transfer matrix relationship of the coupling region C_2 can be expressed as :

$$\begin{pmatrix} E_8 \\ E_6 \end{pmatrix} = \begin{pmatrix} t_2 & k_2 \\ -k_2^* & t_2^* \end{pmatrix} \begin{pmatrix} E_5 \\ E_7 \end{pmatrix} \quad , \qquad (4)$$

where E_6 and E_8 are the complex amplitudes generated when the output coupling region is C_2; t_2 and t_2^* are the self-coupling coefficients of the coupling regions C_2; k_2 and k_2^* are the cross-coupling coefficients of the coupling region C_2.

In the uncoupled region C_3, the relationship between E_9 and E_6 can be expressed as :

$$E_9 = \alpha_{L1}\exp(-j\varphi_{L1}) \cdot \gamma \cdot \alpha_{L4}\exp(-j\varphi_{L4})E_6 \quad , \qquad (5)$$

in the above formula, φ_{L1} and φ_{L4} are the phase changes on the ring waveguide L_1 and L_4 in Fig.1; α_{L_1} and α_{L_4} are representing the transmission coefficients of the ring waveguide L_1 and L_4; E_9 denotes the complex amplitude when entering the coupling region C_3; $\gamma = \alpha_R \exp(j\theta/2)$, where α_R is the transmission loss in the semi-ring waveguide; θ is the phase change in a semi-circular waveguide.

Similarly, the transfer matrix relationship of the coupling region C_3 can be expressed as :

$$\begin{pmatrix} E_{12} \\ E_{10} \end{pmatrix} = \begin{pmatrix} t_3 & k_3 \\ -k_3{}^* & t_3{}^* \end{pmatrix} \begin{pmatrix} E_9 \\ E_{11} \end{pmatrix} \quad , \qquad (6)$$

where E_{10} and E_{12} are representing the complex amplitudes generated when the output coupling region is C_3; E_{11} is representing the complex amplitude generated when the input coupling region is C_3; t_3 and $t_3{}^*$ are the self-coupling coefficients of the coupling regions C_3; k_3 and $k_3{}^*$ are the cross-coupling coefficients of the coupling region C_3.

As for the uncoupled region C_4, there are:

$$E_{13} = \exp[-j(\varphi_3 + \Delta\varphi_3)]E_{12} \quad , \qquad (7)$$

$$E_{15} = \exp[-j(\varphi_4 + \Delta\varphi_4)]E_{10} \quad , \qquad (8)$$

in the above formulas, E_{13} and E_{15} are representing the complex amplitudes generated when the intput coupling region is C_4; φ_3 and φ_4 are the phase changes in the phase shifter and $\varphi_3 + \Delta\varphi_3 = -(\varphi_4 + \Delta\varphi_4)$.

Similarly, the transfer matrix relationship of the coupling region C_4 can be expressed as :

$$\begin{pmatrix} E_{16} \\ E_{14} \end{pmatrix} = \begin{pmatrix} t_4 & k_4 \\ -k_4^* & t_4^* \end{pmatrix} \begin{pmatrix} E_{13} \\ E_{15} \end{pmatrix} \quad , \qquad (9)$$

and there is $E_3 = \alpha_{L1}\exp(j\varphi_{L1}) \cdot \gamma \cdot \alpha_{L4}\exp(j\varphi_{L4})E_{16}$. In the above formulas, E_{14} and E_{16} are representing the complex amplitudes generated when the output coupling region is C_4; t_4 and t_4^* are the self-coupling coefficients of the coupling region C_4; k_4, k_4^* are the cross-coupling coefficients of the coupling region C_4.

After the coupling occurs in the coupling region, the optical signal coupled into the ring waveguide interferes with the optical signal of the ring waveguide. If the two optical signals are in the same direction, they are superimposed during transmission, and the intensity of the optical signal is enhanced when transmitting in the ring waveguide. On the contrary, if the direction of the two optical signals is inconsistent, the two optical signals are canceled during transmission, and the intensity of the optical signal is weakened when transmitting in the ring waveguide.

The Full Width at Half Maximum (FWHM) and quality factor Q are important indicators to measure the performance of microring resonators. The FWHM represents the peak width when the peak height of the output spectral line is half. The smaller the FWHM, the denser the resonance peak at the working wavelength. Since the FWHM is inversely proportional to the quality factor Q, the smaller the FWHM, the larger the quality factor Q, and the stronger the energy storage performance ofthe microring resonator.

From the perspective of energy transfer[11], the optical signal enters the ding-shaped microring resonator from the Input port, and the energy is transmitted along the curved waveguide CW_1. After entering the coupling region C_1, the energy is split. A part of the energy is coupled into the ring waveguide and transmitted. The remaining energy will continue to be transmitted along the curved waveguide CW_1 to the coupling region C_2, and the energy is split again in the coupling region C_2. Most of the energy is coupled into the ring waveguide and transmitted, and the remaining small part of the energy is output from the Through port. When the energy is transmitted to the coupling region C_3, the shunt occurs again. Part of the energy is coupled from the ring waveguide to the curved waveguide CW_2 and transmitted, and the remaining energy continues to transmit along the ring waveguide. When the energy is transmitted to the coupling region C_4, the shunt occurs again, and most of the energy is coupled to the curved waveguide CW_2 and output from the Drop port. The coupling region makes the optical signal undergo multiple energy shunts during transmission. The optical signal that does not satisfy the resonance condition will be directly output, and the optical signal that satisfies the resonance condition will continue to be transmitted in the ring waveguide, which increases the selectivity of the microring to the optical signal.

3 The influence of the number of coupling regions on the output spectral lines

When L_1 = 10 μm, L_2 = 2 μm, L_3 = 15 μm, L_4 = 5 μm, the coupling distance of the coupling region gap is 0.1 μm, x_span=5 μm, y_span=5 μm, the coupling coefficient is 0.289 6, waveguide thickness h=0.22, and the working wavelength is 1.54~1.56 μm, the electric field distribution and transmission spectrum[12] of the standard ding-shaped microring resonator are shown in Fig. 3(color online). When the optical signal is input from the Input port and passes through the coupling region C_1, the electric field satisfying the resonant condition is coupled into the ring and transmitted along the ring waveguide[13-15]. At this time, the Through port has not passed the electric field. According to this mechanism, optical devices with switching function are designed. The remaining electric field continues to transmit along the curved waveguide CW_1.When the optical signal is transmitted to the coupling region C_2, the electric field satisfying the resonance condition is coupled into the ring waveguide and transmitted along the ring waveguide, and the remaining electric field is output through the Through port. When the electric field in the ring is transmitted to the coupling region C_3, the electric field satisfying the resonance condition is coupled out of the ring waveguide and transmitted along the curved waveguide CW_2, while the remaining electric field continues to transmit along the ring waveguide into the coupling region C_4, and the electric field satisfying the resonance condition continues to transmit along the ring waveguide, while the remaining electric field is coupled to the curved waveguide CW_2 and output from the Drop port. The resonance condition can be expressed as :

$$m \cdot \lambda_0 = L \cdot n_{\mathrm{eff}} \quad , \qquad (10)$$

Where m is the resonant series of the microring resonator, λ_0 is the wavelength transmitted in vacuum, L is the circumference of the ring waveguide, and n_{eff} is the effective refractive index. In Fig.3, we can see that after the electric field of the input optical signal passes through the coupling region C_1, most of the electric field is coupled into the ring waveguide and transmitted along the ring waveguide. When passing through the coupling region C_2 and C_3, part of the electric field is transmitted along the ring waveguide, and the other part of the electric field is transmitted to the curved waveguide CW_2.When passing through the coupling region C_4, the electric field in the ring waveguide is partially coupled to the curved waveguide CW_2 and output from the Drop port. The remaining part of the electric field continues to transmit in the ring waveguide until the energy in the ring waveguide tends to be stable, which is consistent with the mechanism of electric field transmission in the micro-ring resonator. From the transmission spectrum of the standard microring resonator, the transmittance of the Through port can reach about 75 %, indicating that the electric field on the curved waveguide CW_1 can be mostly coupled into the ring waveguide in the coupling region C_2. The transmittance of the Drop port can reach 35 %, indicating that part of the electric field continues to resonate in the ring waveguide, and part of the electric field does not satisfy the resonant condition to couple out of the ring waveguide from the Drop port output. From the overall transmission spectrum, the spectral line is relatively stable and smooth, and has good filtering performance.

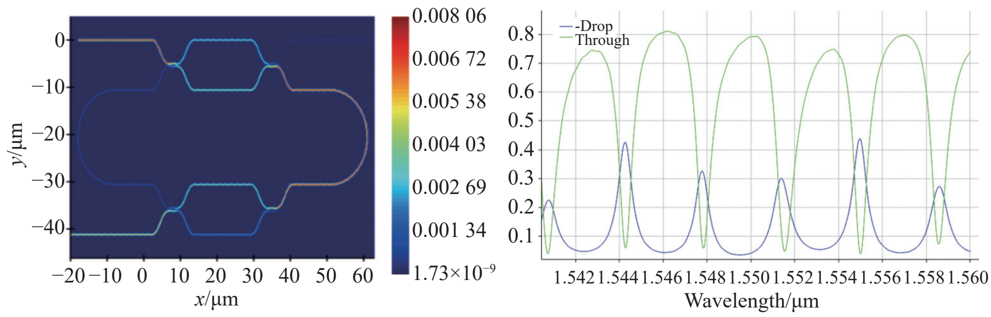

Fig. 3　Electric field distribution and transmission spectrum of standard ding-shaped microring resonator

Fig.4 (color online) shows the electric field distribution of the microring resonator with different numbers of coupling regions. From Fig.4(a), it can be seen that when the ding-shaped micro-ring resonator has only a pair of coupling zones, the electric field is input from the Input port, most of the electric field is coupled into the ring waveguide, and resonance occurs along the ring waveguide. Only part of the unqualified electric field is output from the Drop port. In Fig.4(b), there are two pairs of coupling zones in the ding-shaped microring resonator. The strength of the electric field entering from the Input port decreases. When the coupling occurs in the four coupling zones, most of the electric field can be continuously coupled in the ring waveguide. Only a small part of the electric field does not meet the coupling condition and is output from the Drop port. In Fig.4(c), there are three pairs of coupling zones in the ding-shaped microring resonator. It can be seen from the diagram that when the electric field enters from the Input port, part of the electric field can be coupled into the ring waveguide and resonate all the time, and a small part of the electric field not meeting the resonance condition output from the Drop port.

Fig.5 (color online) shows the output spectra when the wavelength range of the input optical signal is 1.54~1.56 μm, and other parameters are unchanged. When the number of coupling regions is one, two and three pairs respectively, the influence of the number of coupling regions on the output spectral line of the ding-shaped microring resonator is simulated. Fig.5(a) shows that when the ding-shaped microring resonator has only a pair of coupling regions, four resonance peaks are generated in the working band. The transmittance of the Drop port reaches about 40 %, and the transmittance of the Through port reaches about 85 %. The output spectrum lines of the Drop port and Through port are smooth, and the light waves with the wavelength of 1.5428, 1.5445, 1.5532 and 1.5585 μm can be well filtered. It can be seen from Fig.5(b) that when the ding-shaped microring resonator has two pairs of coupling regions, six resonance peaks are generated in the working band. The transmittance of the Drop port reaches about 35 %, and the transmittance of the Through port reaches about 75 %. And the output spectral lines of the Drop port and the Through port are also relatively smooth, which can well filter the light waves with wavelengths of

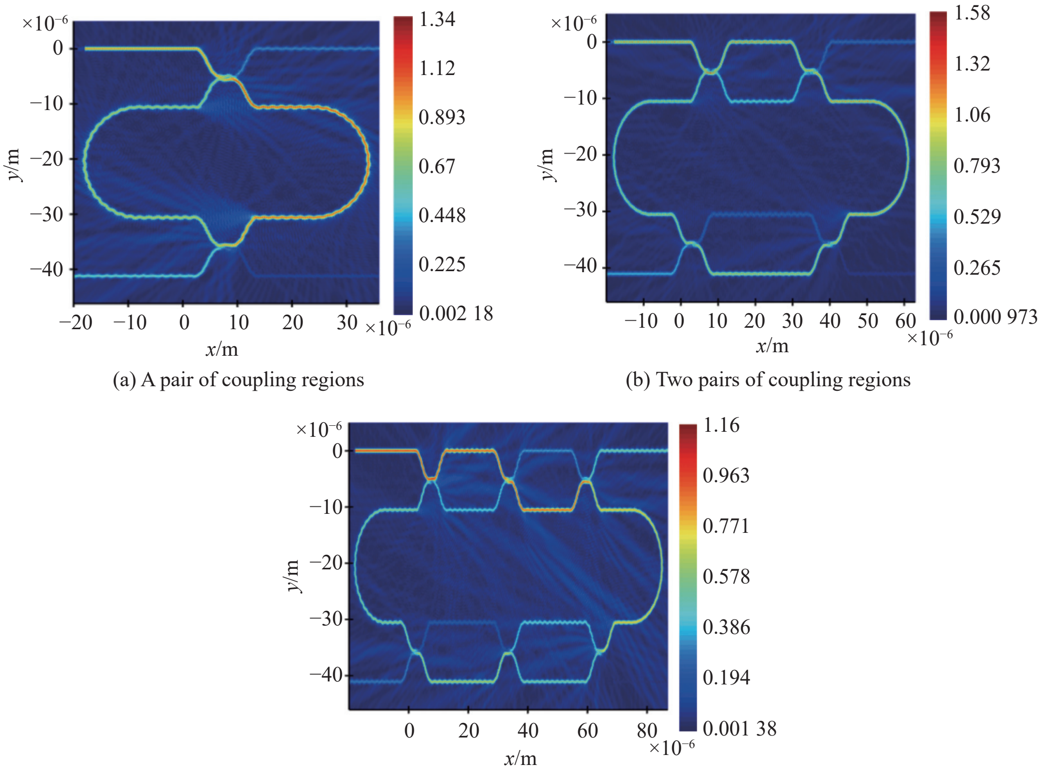

(a) A pair of coupling regions

(b) Two pairs of coupling regions

(c) Three pairs of coupling regions

Fig. 4 Electric field distributions under different coupling regions

1.5402, 1.5445, 1.5478, 1.5514, 1.5550, and 1.5587 μm. It can be seen from Fig.5(c) that when the ding-shaped microring resonator has three pairs of coupling regions, seven resonance peaks are generated in the working band. The transmittance of the Drop port reaches about 38 %, and the transmittance of the Through port reaches about 70 %. And the output spectral lines of the Drop port and the

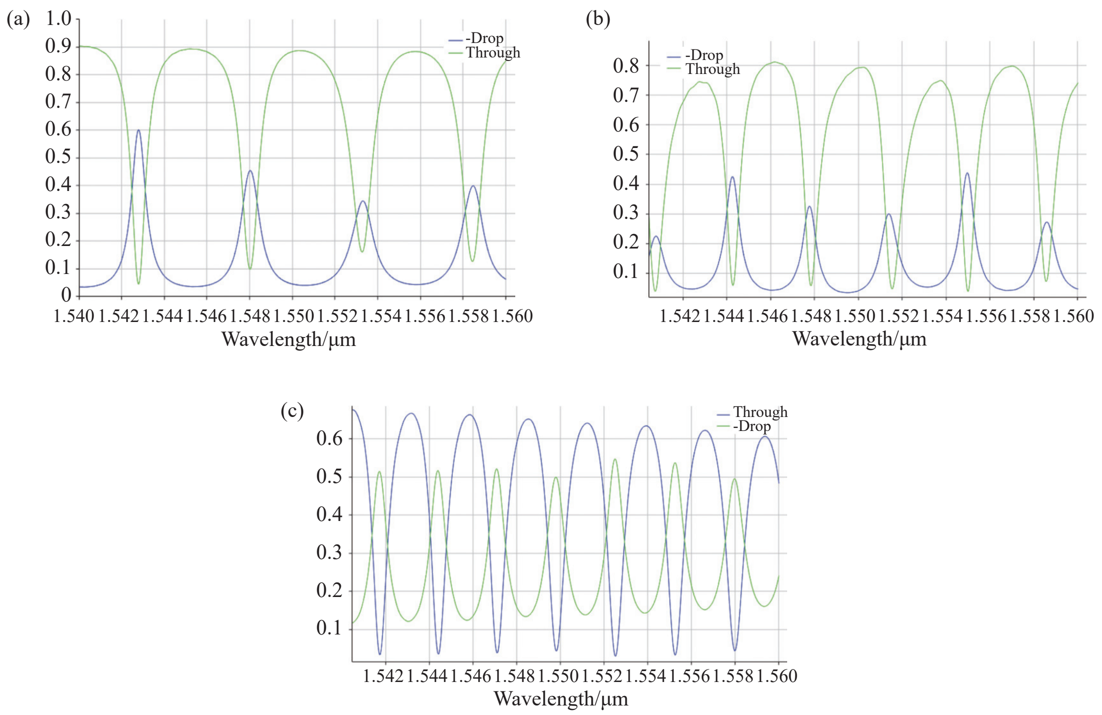

Fig. 5 Output spectra under different numbers of coupling regions. (a) A pair of coupling regions; (b) two pairs of coupling region; (c) three pairs of coupling region

Through port are also relatively smooth, which can well filter the light waves with wavelengths of 1.5415, 1.5445, 1.5472, 1.5498, 1.5526, 1.5558, 1.5580 μm. As shown in Fig.5, due to the fluctuation of the light wave during transmission, the refractive index of the material in the light wave of different wavelengths is also different, and the increase of the coupling region affects the occurrence of two adjacent resonances, so the transmittance of the Drop port and the Through port fluctuates within a certain range.

4 Conclusion

In summary, this paper mainly analyzes the physical model of the ding-shaped microring resonator, and simulates the influence of the number of coupling regions of the ding-shaped microring resonator on the output spectrum. It is found that with the increase of the number of coupling regions of the microring resonator, the number of resonance peaks in the working band of 1.54~1.56 μm increases, which means that the density of resonance peaks in the working band increases, and the FWHM decreases. Due to the inverse relationship between the FWHM and quality factor Q, the larger the quality factor Q, the better the energy storage performance of the microring resonator, and the filtering function on specific wavelengths can be realized.

References:

[1] MARCATILI E A J. Bends in optical dielectric waveguides[J]. *The Bell System Technical Journal*, 1969, 48(7): 2103-2132.

[2] 秦莉, 陆景彬, 马春生, 等. 微环谐振器的弯曲损耗[J]. 半导体光电, 2002, 23(2): 99-102.
QIN L, LU J B, MA CH SH, *et al*.. Bending loss of microring resonators[J]. *Semiconductor Optoelectronics*, 2002, 23(2): 99-102. (in Chinese).

[3] 胡玉洁, 王书晓, 汪大伟, 等. 中红外微环谐振器及应用的研究进展[J]. 激光与光电子学进展, 2020, 57(23): 230004.
HU Y J, WANG SH X, WANG D W, *et al*.. Research progress of mid-infrared micro-ring resonator and its application[J]. *Laser & Optoelectronics Progress*, 2020, 57(23): 230004. (in Chinese).

[4] 王强, 张志琴, 李艳丽. 半径大小对微环谐振器滤波影响的分析[J]. 电子世界, 2019(18): 87-88.
WANG Q, ZHANG ZH Q, LI Y L, *et al*.. Analysis of the influence of the radius size on the micro-ring resonator filter[J]. *Electronic World*, 2019(18): 87-88. (in Chinese)

[5] 刘鑫, 孔梅, 文权. 耦合系数对串联双微环谐振器滤波特性的影响[J]. 中国激光, 2010, 37(11): 2885-2890.
LIU X, KONG M, WEN Q. Influence of coupling coefficients on filtering characteristics of series coupled two-microring resonators[J]. *Chinese Journal of Lasers*, 2010, 37(11): 2885-2890. (in Chinese).

[6] 冯松, 高勇. SiGe-OI 微环谐振器的滤波特性分析[J]. 西安理工大学学报, 2016, 32(4): 443-448.
FENG S, GAO Y. Analysis of the filtering property of SiGe-OI micro-ring resonator[J]. *Journal of Xi'an University of Technology*, 2016, 32(4): 443-448. (in Chinese).

[7] SACHER W D, GREEN W M J, GILL D M, *et al*.. Binary phase-shift keying by coupling modulation of microrings[J]. *Optics Express*, 2014, 22(17): 20252-20259.

[8] 李昕娟. 微环谐振器的耦合和特性的分析与研究[D]. 兰州: 兰州交通大学, 2015.
LI X J. Analysis and Research on Coupling and Characteristics of Microring resonators[D]. Lanzhou: Lanzhou Jiaotong University, 2015. (in Chinese).

[9] 张小贝, 黄德修, 洪伟, 等. 传输矩阵法分析微环谐振器阵列传输特性[J]. 光学学报, 2007, 27(9): 1585-1592.
ZHANG X B, HUANG D X, HONG W, *et al*.. Transfer matrix method for analyzing transmission characteristics of microring resonator arrays[J]. *Acta Optica Sinica*, 2007, 27(9): 1585-1592. (in Chinese).

[10] 薛寒. 基于微环谐振器的光子器件研究[D]. 秦皇岛: 燕山大学, 2021.
XUE H. *Research on photonic devices based on microring resonator*[D]. Qinhuangdao: Yanshan University, 2021. (in Chinese).

[11] LI X J, WU R, HU Y F, *et al*.. Study of energy transfer in silicon-based micro-ring resonators[J]. *Optoelectronics Letters*, 2014, 10(5): 321-324.

[12] 李锋, 张静. 微环谐振器传输特性分析[J]. 科学技术与工程, 2012, 12(36): 9971-9975.
LI F, ZHANG J. Transmission characteristics of microring resonator[J]. *Science Technology and Engineering*, 2012, 12(36): 9971-9975. (in Chinese).

[13] 穆洲. 基于微环谐振器的传输特性及温度传感特性研究[D]. 兰州: 兰州交通大学, 2020.
MU ZH. *Research on transmission characteristics and temperature sensing characteristics based on microring resonator*[D]. Lanzhou: Lanzhou Jiaotong University, 2020. (in Chinese).

[14] 史振江, 李志全, 陆飞. 硅基波导微环谐振腔光学传输特性研究[J]. 传感器世界, 2020, 26(8): 7-11.
SHI ZH J, LI ZH Q, LU F. Research on optical transmission characteristics of microring resonator with silicon waveguide[J]. *Sensor World*, 2020, 26(8): 7-11. (in Chinese).

[15] 南午申申. 微环谐振腔的传输特性分析[J]. 工程与试验, 2021, 61(4): 9-11.
NAN W SH SH. Analysis of transmission characteristics of microring resonator[J]. *Engineering & Test*, 2021, 61(4): 9-11. (in Chinese).

Author Biographics:

Wu Rong (1968—), female, born in Wuwei, Gansu Province, Professor, School of Electronic and Information Engineering, Lanzhou Jiaotong University. Her research interest is on semiconductor integrated circuit. E-mail: 759165367@qq.com

Zhang Hao-chen (1997—), male, born in Dingxi, Gansu Province, postgraduate, School of Electronic and Information Engineering, Lanzhou Jiaotong University. His research is on potical devices. E-mail: 2651809834@qq.com